HOKKAIDO UNIVERSITY

Title	Hypothesis on particle structure and assembly of rice dwarf phytoreovirus: interactions among multiple structural proteins
Author(s)	Ueda, Shigenori; Masuta, Chikara; Uyeda, Ichiro
Citation	Journal of General Virology, 78, 3135-3140 https://doi.org/10.1099/0022-1317-78-12-3135
Issue Date	1997
Doc URL	http://hdl.handle.net/2115/5819
Type	article
File Information	JGV78.pdf

Instructions for use

Hypothesis on particle structure and assembly of rice dwarf phytoreovirus: interactions among multiple structural proteins

Shigenori Ueda, Chikara Masuta and Ichiro Uyeda

Laboratory of Plant Virology and Mycology, Department of Agrobiology and Bioresources, Faculty of Agriculture, Hokkaido University, Sapporo 060, Japan

To study the morphogenesis and packaging of rice dwarf phytoreovirus (RDV), the interactions among multiple structural proteins were analysed using both the yeast two-hybrid system and far-Western blotting analysis. The following protein–protein interactions were observed. P3 (major core protein) bound to itself as well as to P7 (nucleic acid-binding protein) and P8 (major outer capsid protein). P7 bound to P1 (RNA-dependent RNA polymerase) and P8, in addition to P3. Based on these findings, we hypothesize that the core shell structure is based on P3–P3 interactions and that P7 has the ability to bind to multiple structural proteins as well as to genomic RNAs during viral particle assembly. Based on the observed protein–protein interactions and on computer-aided analysis of the numbers of structural proteins per particle, possible RDV assembly events are proposed.

The genome of rice dwarf phytoreovirus (RDV), a member of the family *Reoviridae*, consists of 12 dsRNAs segments, of which one copy of each is presumed to be packaged into a virion (Anzola *et al.*, 1987). All the structural and non-structural proteins have been identified and assigned to the genomic segments (Suzuki *et al.*, 1994; Murao *et al.*, 1994). RDV has an icosahedral structure of about 70 nm in diameter (Uyeda & Shikata, 1982). After treatment with an organic solvent such as CCl_4, the purified viral particles are mainly composed of proteins P1, P3, P7 and P8. Without such treatment two additional proteins, P2 and P5, are present. P8, a major outer capsid protein, is also easily removed from the core particles by $MgCl_2$ treatment (Omura *et al.*, 1989). The core particles include P1, P3, P7, dsRNAs, and P5, a possible guanyltransferase (Suzuki *et al.*, 1996). P3 is a major core capsid protein, and P1 is an RNA-dependent RNA polymerase (Suzuki *et al.*, 1992). Recently, we found by Northwestern blotting assay that P7 was the second major core component

and has non-specific nucleic acid-binding activity (Ueda & Uyeda, 1997).

Little is known about the replication and assembly process of RDV or about interactions among multiple structural proteins in viral particles. Therefore, in this study, we investigated protein–protein interactions in order to gain a better understanding of viral morphogenesis and the assembly process. To our knowledge, this is the first model of the assembly of plant viral proteins and RNAs based on observations of protein–protein interactions, using the yeast two-hybrid system and far-Western blotting analysis.
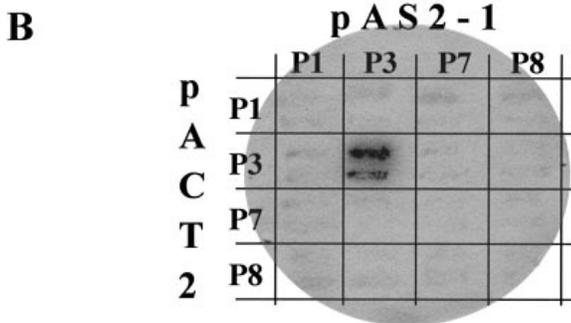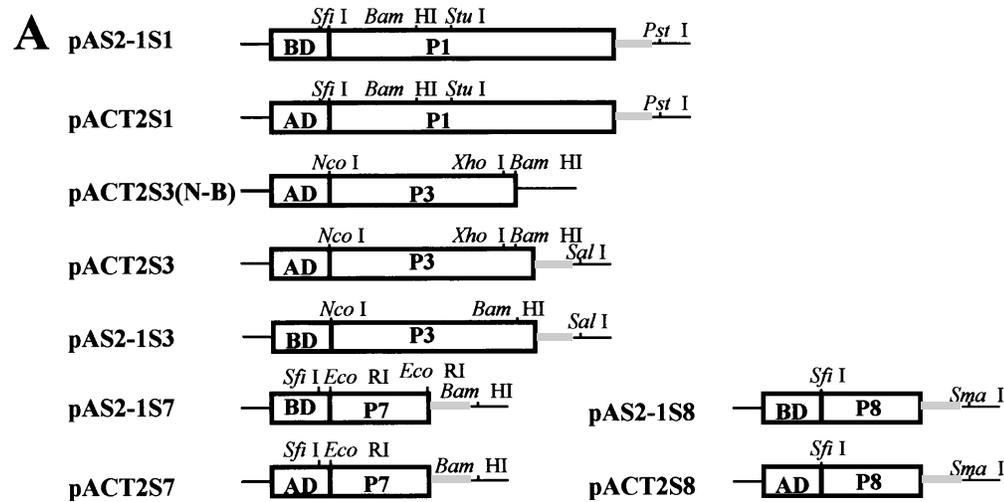
For the yeast two-hybrid system and far-Western blotting analysis, the PCR template cDNA clones, pRDTN1, pRDS3 and pRDS8 and pMALRDANS7 (Ueda & Uyeda, 1997) were constructed. Ex *Taq* DNA polymerase (Takara) was used to amplify DNA with appropriate primers based on the known nucleotide sequences of S1 (Suzuki *et al.*, 1992), S3 (Yamada *et al.*, 1990), S7 (Nakashima *et al.*, 1990) and S8 (Omura *et al.*, 1989). For the yeast two-hybrid system, plasmids pAS2-1 and pACT2 were purchased from Clontech. pAS2-1 encodes the DNA-binding domain (BD) protein and contains a selection marker for tryptophan-defective (Trp⁻) auxotrophy. pACT2 encodes the DNA-activation domain (AD) protein and contains a selection marker for leucine-defective (Leu⁻) auxotrophy. PCR products were cleaved with appropriate restriction enzymes and cloned into pAS2-1 and pACT2 (Fig. 1A). For far-Western blotting analysis, pMAL-c2 (New England Biolabs) was used to produce maltose binding protein (MBP)-fused proteins in *E. coli* DH5α or HB101 strains. Constructions of all the clones was confirmed by sequencing using a Li-Cor DNA sequencer or Western blotting assay.

For the yeast two-hybrid system, *Saccharomyces cerevisiae* Y187 was used for expression of viral proteins. Yeast cells were grown by the conventional method. Transformation of yeast cells was performed by the lithium acetate method according to Rose *et al.* (1990) with incubation for 2–3 days at 30 °C. To investigate protein–protein interactions, positive colonies were detected by using 5-bromo-4-chloro-3-indolyl β-D-galactopyranoside (X-Gal) after freezing the filters with liquid nitrogen according to the manufacturer's protocol.

For far-Western blotting, viral proteins were separated in 8% SDS–polyacrylamide gels (Laemmli, 1970) and blotted

Author for correspondence: Ichiro Uyeda.

Fax +81 11 716 0879. e-mail uyeda@res.agr.hokudai.ac.jp

A

pAS2-1S1 — BD | P1 (Sfi I, Bam HI, Stu I; Pst I)

pACT2S1 — AD | P1 (Sfi I, Bam HI, Stu I; Pst I)

pACT2S3(N-B) — AD | P3 (Nco I; Xho I, Bam HI)

pACT2S3 — AD | P3 (Nco I; Xho I, Bam HI; Sal I)

pAS2-1S3 — BD | P3 (Nco I; Bam HI; Sal I)

pAS2-1S7 — BD | P7 (Sfi I, Eco RI, Eco RI; Bam HI)   pAS2-1S8 — BD | P8 (Sfi I; Sma I)

pACT2S7 — AD | P7 (Sfi I, Eco RI; Bam HI)   pACT2S8 — AD | P8 (Sfi I; Sma I)

B

p A S 2 - 1 : P1, P3, P7, P8 (columns)
p A C T 2 : P1, P3, P7, P8 (rows)

C

		pAS2-1				
		P1	P3	P7	P8	Cont**
pACT2	P1	-	-	-	-	-
	P3	-	++++	-	-	+/-
	P7	-	-	-	-	-
	P8	-	-	-	-	-
	Cont*	+/-	-	+/-	-	

Fig. 1. The yeast two-hybrid system analysis. (A) Construction of recombinant plasmids. A series of cDNA clones derived from the viral RNAs were constructed in plasmid pAS2-1 or pACT2 downstream of the binding domain protein gene (BD). Oligonucleotide primers for amplification of PCR products were derived from the nucleotide sequences of the segments. pAS2-1S1 and pACT2S1 contain a cDNA fragment from the initiation codon to the 3′ terminus of S1. pBluescriptS1(B-P) and pAS2-1S1(B-P) were created by inserting a BamHI (nt 1518)–PstI fragment of pRDTN1 at an appropriate polylinker region of pBluescript SK(−) or pAS2-1. pACT2S1(B-P) was created by inserting a BamHI–SalI fragment of pBluescriptS1(B-P) between the BamHI and XhoI sites in pACT2. pAS2-1S1 and pACT2S1 were created by inserting a SfiI–StuI (nt 2020) fragment from the PCR products generated from pRDTN1 in pAS2-1S1(B-P) or pACT2S1(B-P). pACT2S3 and pAS2-1S3, which contain a cDNA fragment from the initiation codon to the 3′ terminus of S3, were also constructed in two steps. First, pAS2-1S3(N-B) and pACT2S3(N-B) were created by inserting a NcoI–BamHI (nt 3068) fragment from the PCR products generated from pRDS3. Then, a XhoI (nt 2935)–SalI fragment was isolated from pRDS3 and inserted between two XhoI sites in pACT2S3(N-B) to create pACT2S3. pAS2-1S3 was created by inserting a BamHI–SalI fragment from pACT2S3 between BamHI and SalI in pAS2-1S3(N-B). Likewise, the other recombinant plasmids were constructed as follows. pAS2-1S7, EcoRI fragment PCR-amplified from pMALRDANS7 in pAS2-1; pACT2S7, SfiI–BamHI fragment from pAS2-1S7 in pACT2; pAS2-1S8 and pACT2S8, SfiI–SmaI fragment PCR-amplified from pRDS8 in pAS2-1 and pACT2; The grey line represents the non-coding sequence regions derived from each RDV segments. (B) The β-galactosidase filter assay using the yeast two-hybrid system. Cotransformation was performed by the lithium acetate method, and incubation was carried out on tryptophan-defective (Trp⁻) and leucine-defective (Leu⁻) synthetic dropout (SD) plates. The colonies containing each plasmid were streaked on the SD plate to obtain colonies harbouring both recombinant pAS2-1 and pACT2. Positive signals on the filter were visualized with X-Gal after freezing the filter with liquid nitrogen. (C) The results of the assays are summarized with control colonies having a single plasmid selected on Trp⁻ (*) or Leu⁻ (**) SD plates.

onto Hybond-C membrane (Amersham). After incubating the membranes in a solution of MBP-fused proteins, the viral proteins were probed with antiserum to MBP and then with goat anti-rabbit IgG(H+L)–alkaline phosphatase (AP), or with anti-MBP enzyme conjugate containing 5 mM $MgCl_2$. Signals were developed with nitro blue tetrazolium (NBT) and 5-bromo-4-chloro-3-indolyl phosphate (BCIP).

To analyse the molecular ratio among structural proteins in the purified virus, viral proteins were separated in 8% SDS–polyacrylamide gels and stained with Coomassie Brilliant Blue. The densitometric assay was performed with an image analyser. After the separated proteins were scanned into a computer, we calculated the molecular ratio among multiple structural proteins using the computer program NIH image
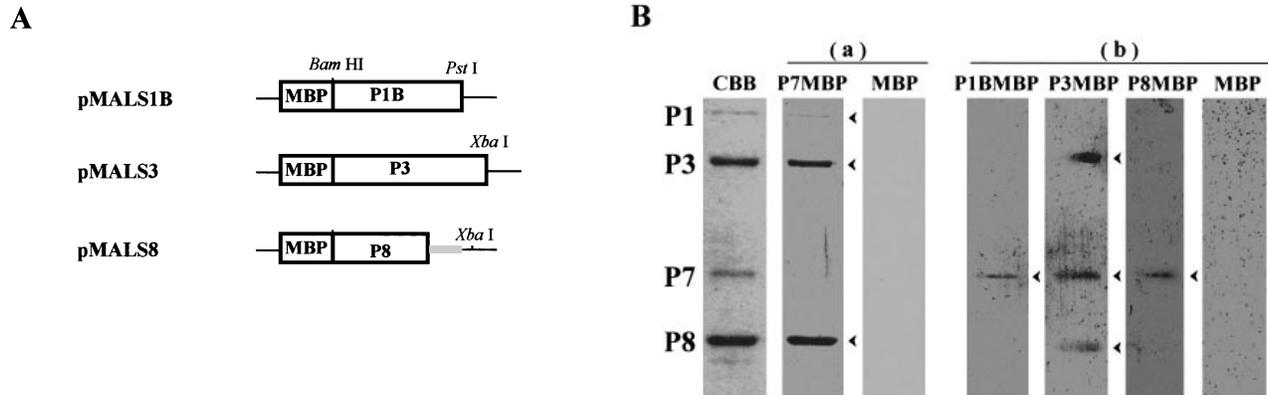
A

B

Fig. 2. Far-Western blotting analysis. (A) Construction of recombinant plasmids. pMALS1B was constructed by inserting half of the S1 fragment (nt 1517–4370) corresponding to the C-terminal half of the P1 open reading frame sequence (ORFs) in pMAL-c2. pMALS3 was constructed by inserting a fragment (nt 39–3098) of the P3 full-length ORFs in pMAL-c2. pMALS8 was constructed by inserting a fragment (nt 24–3′ terminus) of P8 full-length ORFs in pMAL-c2. pMALRDANS7 was previously described by Ueda & Uyeda (1997). The grey line is as in Fig. 1 (A). (B) Far-Western blotting assay using antiserum against maltose binding protein (MBP). Purified RDV (0·5 μg) was separated by 8% SDS–PAGE. The gels were stained with Coomassie Brilliant Blue (CBB) or were electrically transferred onto nitrocellulose membranes. The membranes were incubated in 10–15 μg/ml of MBP-fused proteins in TBS (50 mM Tris–HCl, pH 7·5, 150 mM NaCl) containing 5% skim milk (TBSM) with gentle shaking overnight at 6 °C followed by blocking in TBSM for 2 h at 37 °C. After washing three times with TBS containing 0·1% Triton X-100 (TBST) and twice with TBS, the membranes were incubated for 2 h at 37 °C with antiserum to MBP in TBSM or enzyme conjugate of anti-MBP γ-globulin and alkaline phosphatase (AP) in TBSM containing 5 mM $MgCl_2$. When antiserum was used, after washing, the membranes were subsequently probed with goat anti-rabbit IgG(H+L)–AP (Zymed) for 2 h at 37 °C in TBSM. Signals were developed with nitro blue tetrazolium (NBT) and 5-bromo-4-chloro-3-indolyl phosphate (BCIP). (*a*) The membranes were first probed with MBP-fused P7 (P7MBP) or MBP (control), followed by anti-MBP serum, and then with goat anti-rabbit–AP conjugate. (*b*) The membranes were probed with MBP–the C-terminal half of P1 including a GDD motif (P1BMBP), MBP–P3 (P3MBP), MBP–P8 (P8MBP), or MBP (control), and treated with an enzyme conjugate of γ-globulin against MBP.

version 1.56. The results were analysed for significance using the χ^2 test.

To investigate protein–protein interactions, we constructed recombinant expression vectors containing genes of RDV structural proteins for use in the yeast two-hybrid system (Fig. 1A). The viral genes were inserted downstream of the BD protein gene in pAS2-1 or the AD protein gene in pACT2. The junctions around the inserted segments were confirmed for correct orientation by sequencing. One of the results of the two-hybrid assays is shown in Fig. 1(B), and all the results are summarized in Fig. 1(C).

A blue signal from the β-galactosidase filter assay for protein–protein interactions was detected only with the combination P3–P3. To further investigate the binding affinity between the P3 subunits, we used recombinant plasmid pACT2S3(N-B), containing a C-terminal, 7-amino-acid truncated P3 gene (Fig. 1A). The signal with the combination of pACT2S3(N-B) and pAS2-1S3 was significantly weaker than that with the combination of pACT2S3 and pAS2-1S3 (data not shown). This result suggest that the deleted C terminus of P3 might be involved in the P3–P3 interaction, although further experiments are needed to clarify this. It was considered that authentic proteins should be mimicked as much as possible, because the *in vivo* structural constraint to maintain viral morphology must affect the protein–protein interactions; otherwise, the particle cannot maintain a rigid shape. Conse-

quently, we decided to perform a far-Western blotting assay, which has recently been successfully used for monitoring protein–protein interactions (Ye & Baltimore, 1994; Miyao *et al.*, 1996).

For this purpose, we constructed MBP-fused protein expression plasmids (Fig. 2A), and purified MBP-fusion proteins were used as probes to analyse interactions with purified RDV structural proteins. All the purified MBP-fusion proteins had the correct molecular mass, as estimated by SDS–PAGE, and they reacted with antisera against RDV or against MBP (data not shown). Using antiserum against MBP, P7–MBP appeared to bind strongly to P3 and P8, and weakly to P1; MBP did not bind to any viral proteins [Fig. 2B(*a*)]. When other fusion proteins were used as probes, however, no specific signals were obtained. To improve the specificity of the antibody, anti-MBP γ-globulin–AP conjugate was made and added to the hybridization mixture, containing $MgCl_2$ at a final concentration of 5 mM. As shown in Fig. 2B(*b*), P1B–MBP fusion protein was found to bind to P7. Likewise, P3–MBP was able to bind to P3, P7 and P8. Although P8–MBP could bind to P7, P8–P8 interactions were not detected.

The molecular ratio among the multiple structural proteins in purified virus was estimated by computer-aided analysis. As RDV has a $T = 9$ icosahedral structure and there are 92 channels surrounded by 180 morphological units on the virus
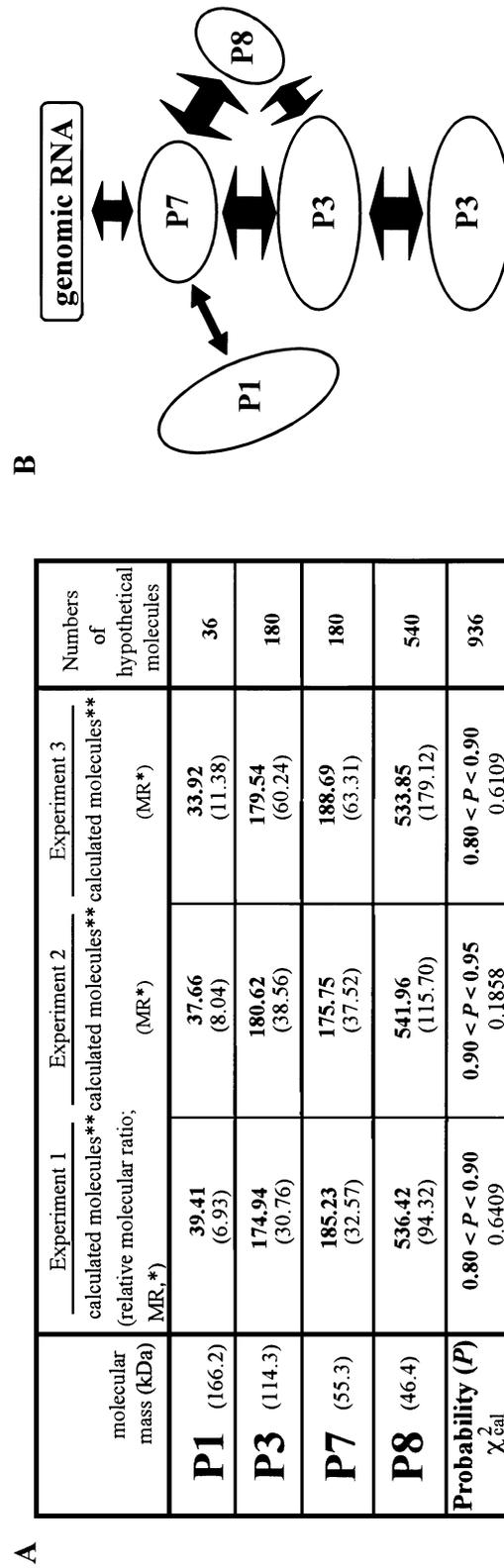
A

molecular mass (kDa)	Experiment 1	Experiment 2	Experiment 3	Numbers of hypothetical molecules
	calculated molecules** (relative molecular ratio; MR,*)	calculated molecules** (MR*)	calculated molecules** (MR*)	
P1 (166.2)	39.41 (6.93)	37.66 (8.04)	33.92 (11.38)	36
P3 (114.3)	174.94 (30.76)	180.62 (38.56)	179.54 (60.24)	180
P7 (55.3)	185.23 (32.57)	175.75 (37.52)	188.69 (63.31)	180
P8 (46.4)	536.42 (94.32)	541.96 (115.70)	533.85 (179.12)	540
Probability (P) χ^2_{cal}	0.80 < P < 0.90 0.6409	0.90 < P < 0.95 0.1858	0.80 < P < 0.90 0.6109	936

B

Fig. 3. Relationship among RDV structural proteins. (A) Computer-aided molecular ratio analysis. The relative molecular ratio (MR,*) is the value of the protein area/protein molecular mass. The calculated molecules (**) is (the value of the MR of the protein/sum of the MR) × 936. 936 is the sum of the numbers of hypothetical molecules. (B) Protein–protein interactions with genomic RNA. The interaction between P7 and genomic RNA was described by Ueda & Uyeda (1997).

capsid (Uyeda & Shikata, 1982), we hypothesize that the numbers of molecules on P1, P3, P7 and P8 per particle are 36, 180, 180 and 540, respectively. The results from three independent experiments indicate that this ratio is statistically significant (Fig. 3 A).

To understand the morphogenesis of RDV, we have demonstrated protein–protein interactions among multiple structural proteins using the yeast two-hybrid system and far-Western blotting analysis. Previously, we have shown, by Northwestern blotting assay and caesium trifluoroacetate (CsTFA) density gradient centrifugation, that P7 possesses nonspecific nucleic acid-binding activity. After centrifugation, P7 plus genomic dsRNAs (P7–dsRNA) and the open core particles, which are composed of P1, P3 and P7, are fractionated (Ueda & Uyeda, 1997). We believe that these cofractionated proteins have protein–protein interactions in the viral particle.

In the yeast two-hybrid system, only P3–P3 interactions were detected among all of the combinations of viral structural proteins (Fig. 1 B, C), suggesting that this interaction is very stable and has a significant role in supporting the core shell structure. The far-Western blotting assay also showed interactions between P1–P7, P3–P7, P3–P8 and P7–P8 in addition to P3–P3 (Fig. 2 B). All protein–protein interactions found are summarized in Fig. 3 (B). Interestingly, P7 was found to bind to three other structural proteins. We previously observed that a reduced amount of P8 bound to a complex of P7–dsRNA more tightly than P3 after CsTFA centrifugations. (Ueda & Uyeda, 1997). Although we had expected some P8–P8 interactions, since P8 is an outer capsid protein forming the capsomere, in far-Western blotting the signal for P8–P8 interaction did not reach a detectable level. Given the mass of the unit capsomere, a capsomere is thought to contain three molecules of P8 (Omura et al., 1989). The P8–P8 interaction perhaps exists in a virion; P8–P8 and P8–P3 interactions are thought to be relatively weak because P8 is easily dissociated from the core particles by treatment with $MgCl_2$.

The ratio of P1:P3:P7:P8 is estimated to be 36:180:180:540 as determined by computer-aided analysis (Fig. 3 A). Therefore, one particle should contain approximately 180 molecules of P3, P7 and P8 trimers. Based on this molecular ratio and on the protein–protein interactions described in this paper, we propose a hypothesis on RDV particle structure and assembly. As the RDV particle has a $T = 9$ arrangement, the outer capsid capsomeres, the surface arrangement of P8 trimers includes pentagonal and hexagonal arrays. There are 12 channels at the centre of the pentamers and 20 channels at the centre of the hexamers. In order to interact P7 with P3 and P8 together, P7 forms into a certain structure, possibly a tetrahedron that is integrated as a part of the inner core layer. Although we did not detect P7–P7 interaction, we believe that another protein layer built up by P7–dsRNA should exist under the P3 core shell. P7–dsRNA could bind to P3 at the hole sites so that P7 would directly bind to P8 on the P3 core shell. According to a previous report (Inoue & Timmins, 1985),

genomic RNAs are thought to exist within a radius of 23 nm from the centre of the particle, and they must bind to P7, hanging inward. Since P1 only interacts with P7 and the particle contains 12 channels at the centre of the pentamers and 20 channels at the hexamers consisting of P8 trimers as capsomeres, we speculate that monomeric or dimeric P1 is associated with each channel. Alternatively, a trimer of P1 could be associated with each of 12 channels at the centre of the pentamers. Although we have not yet analysed other viral structural proteins such as P2 and P5, these proteins should also be integrated in the RDV particle. In fact, we think that P5, a possible guanyltransferase (Suzuki et al., 1996), may be located near the channels, as this protein is thought to be associated with P1, the RNA polymerase.

As summarized in Fig. 3 (B), P7 seems to play an important role as a 'hinge' for the assembly of viral structural proteins and genomic RNA. Besides its function in particle assembly, P7 may also contribute to the replication of viral RNAs as an accessory factor, because of the protein–protein interaction between P7 and P1.

It is difficult to compare our hypothesis to those for of other members of Reoviridae, because RDV has a $T = 9$ structure while the other reoviruses investigated, such as rotaviruses (Patton, 1995), mammalian reoviruses (Nibert et al., 1996) and orbiviruses (Roy, 1996), have a $T = 13$ structure. In some cases, however, they share similar properties; for example, polymerases are located near channels (Nibert et al., 1996) and a core particle is surrounded by protein units of trimers (Patton, 1995; Roy, 1996).

In this paper, we have described some interactions among the structural proteins P1, P3, P7 and P8, and RDV assembly events were hypothesized based on these interactions. However, at this stage, it is not clear to what degree these in vitro interactions reflect authentic protein–protein interactions in the particle. Further experiments using E. coli-expressed viral proteins are underway for in vitro reconstitution of the RDV particle.

References

Anzola, J. V., Xu, Z., Asamizu, T. & Nuss, D. (1987). Segment-specific inverted repeats found adjacent to conserved terminal sequences in wound tumor virus genome and defective interfering RNAs. *Proceedings of the National Academy of Sciences, USA* **84**, 8301–8305.

Inoue, H. & Timmins, P. A. (1985). The structure of rice dwarf virus determined by small-angle neutron scattering measurements. *Virology* **147**, 214–216.

Laemmli, U. K. (1970). Cleavage of structural proteins during the assembly of the head of bacteriophage T4. *Nature* **227**, 680–685.

Miyao, T., Yasui, K., Sakurai, H., Yamagishi, M. & Ishihama, A. (1996). Molecular assembly of RNA polymerase from the fission yeast *Schizosaccharomyces pombe*: subunit-subunit contact network involving Rpb5. *Genes to Cells* **1**, 843–854.

Murao, K., Suda, N., Uyeda, I., Isogai, M., Suga, H., Yamada, N., Kimura, I. & Shikata, E. (1994). Genomic heterogeneity of rice dwarf phytoreovirus field isolates and nucleotide sequences of variants of genome segment 12. *Journal of General Virology* **75**, 1843–1848.

Nakashima, K., Kakutani, T. & Minobe, Y. (1990). Sequence analysis and product assignment of segment 7 of the rice dwarf virus genome. *Journal of General Virology* **71**, 725–729.

Nibert, M. L., Schiff, L. A. & Fields, B. N. (1996). Reoviruses and their replication. In *Fields Virology*, 3rd edn, pp. 1557–1596. Edited by B. N. Fields, D. M. Knipe & P. M. Howley. Philadelphia: Lippincott–Raven.

Omura, T., Ishikawa, K., Hirano, H., Ugaki, M., Minobe, Y., Tsuchizaki, T. & Kato, H. (1989). The outer capsid protein of rice dwarf virus is encoded by genome segment S8. *Journal of General Virology* **70**, 2759–2764.

Patton, J. T. (1995). Structure and function of the rotavirus RNA-binding proteins. *Journal of General Virology* **76**, 2633–2644.

Rose, M. D., Winston, F. & Hieter, P. (1990). *Methods in Yeast Genetics: A Laboratory Course Manual*. Cold Spring Harbor, NY: Cold Spring Harbor Laboratory.

Roy, P. (1996). Orbivirus structure and assembly. *Virology* **216**, 1–11.

Suzuki, N., Tanimura, M., Watanabe, Y., Kusano, T., Kitagawa, Y., Suda, N., Kudo, H., Uyeda, I. & Shikata, E. (1992). Molecular analysis of rice dwarf phytoreovirus segment S1: interviral homology of the putative RNA-dependent RNA polymerase between plant- and animal-infecting reovirus. *Virology* **190**, 240–247.

Suzuki, N., Sugawara, M., Kusano, T., Mori, H. & Matsuura, Y. (1994). Immunodetection of rice dwarf phytoreoviral proteins in both insect and plant hosts. *Virology* **202**, 41–48.

Suzuki, N., Kusano, T., Matsuura, Y. & Omura, T. (1996). Novel NTP binding property of rice dwarf phytoreovirus minor core protein P5. *Virology* **219**, 471–474.

Ueda, S. & Uyeda, I. (1997). The rice dwarf phytoreovirus structural protein P7 possesses non-specific nucleic acids binding activity *in vitro*. *Molecular Plant Pathology On-Line* [http://www.bspp.org.uk/mppol/) 1997/0123uyeda.

Uyeda, I. & Shikata, E. (1982). Ultrastructure of rice dwarf virus. *Annals of the Phytopathological Society of Japan* **48**, 295–300.

Yamada, N., Uyeda, I., Kudo, H. & Shikata, E. (1990). Nucleotide sequence of rice dwarf virus segment 3. *Nucleic Acids Research* **18**, 6419.

Ye, Z. S. & Baltimore, D. (1994). Binding of Vav to Gab2 through dimerization of Src homology 3 domains. *Proceedings of the National Academy of Sciences, USA* **91**, 12629–12633.